Hindawi
International Journal of Antennas and Propagation
Volume 2022, Article ID 5379071, 9 pages
https://doi.org/10.1155/2022/5379071

Research Article

Investigation of Multibeam Forming Algorithm for Cylindrical Conformal Array Antenna

Ke Zhao,[1] **Lizhe Liu**,[1,2] **and Lirong Mei**[1,2]

[1]*The 54th Research Institute of CETC (CETC-54), Shijiazhuang, China*
[2]*Science and Technology on Communication Networks Laboratory, Shijiazhuang, China*

Correspondence should be addressed to Lizhe Liu; zk_879785757@163.com

Received 6 January 2022; Revised 15 March 2022; Accepted 21 March 2022; Published 28 March 2022

Academic Editor: Mohammad Alibakhshikenari

A multibeam forming algorithm based on cylindrical conformal array antenna is proposed in this paper. A comprehensively optimized algorithm of Taylor weights is used to reduce sidelobes. Multiple beams pointed at different azimuth angles are formed based on a reconfigurable overlapping array division method of subarrays, therefore each beam can get the maximum excitation of subarrays and ensure the pointing accuracy of the main lobe. Finally the cylindrical array antenna realizes the multibeam scanning and area coverage. The experimental results show that the sidelobe level after comprehensive optimization is 7.37 dB lower than that without optimization and 1.71 dB lower than that of traditional optimization when a single beam is formed. The comprehensive optimization can eliminate the grating lobe between two beams and reduce the sidelobe to -15 ~ -20 dB when the two beams are 30°. The left sidelobe is reduced by 2.75 dB and the right sidelobe is reduced by 1.69 dB after comprehensive optimization when the two beams are separated by 40°.

1. Introduction

The phased array antenna adjusts the weighting parameters of each element to achieve noise filtering from the input data compared with an antenna element of low gain and weak directivity. The optimal spatial filtering can be realized by forming a null steering stuffing in the interference direction and obtaining the maximum gain in the desired direction. Meeting the requirements of high gain, multidirectional and specific working environment, the performance of the wireless communication system can be further improved [1,2]. The limited spatial coverage and inflexible beam direction of traditional array antenna make the conformal antennas become a new research focus [3].

The conformal antenna has the same spatial characteristics as the carrier compared with traditional array antenna, which will not reduce the aerodynamic performance of the original carrier. The conformal array carrier has smaller radar cross section (RCS) and is more convenient for stealth design compared with the same aperture size planar array [4–6]. In addition, the special shape of conformal antenna attached to the carrier surface makes the carrier higher space utilization. Meanwhile, it has a larger beam coverage and more flexible beam pointing ability to realize multitarget tracking and scanning. Nevertheless, the radiation directions of conformal array elements are inconsistent due to the influence of the curvature change of the carrier. The cross-polarization isolation between array elements clearly deteriorated when scanning at a large angle [7, 8]. The conformal array with special structure has shadow effect while transmitting and receiving beams. Thus the conformal array is divided into sub-array areas and forming beams in different directional airspace [9]. For common conformal arrays, cylindrical array [10], conical array [11], spherical array [12] and circular array [13] can all realize 360° omnidirectional scanning. However, the mutual coupling effect and cross-isolation between array elements make the computational complexity of conical array and spherical array too high, which is not conducive for engineering realization. The physical structure and mathematical model of the cylindrical array are the simplest among conformal arrays for omnidirectional scanning. Meanwhile, the reception and

transmission of a single beam cannot meet the increasingly complex electromagnetic environment and task requirements under the demand of multitarget tracking in the whole airspace [14], therefore the multibeam forming of cylindrical array antenna is studied.

The influence of wavefront curvature will lead to the elevation of sidelobe and the deviation of beam-pointing when conformal array is used for beamforming. The interaction between two beams results in sidelobe lifting and grating lobes while forming multiple beams. In order to eliminate this disadvantage, it is necessary to optimize the beamforming algorithm of conformal array [15–17]. In [18], the authors addressed a constrained multiobjective problem of sparse conformal array design. In [19], the author proposed an optimization method based on genetic algorithm and convex optimization to solve the problem of high sidelobe level of circular array. In [20], a beam design method based on radial basis function neural network is proposed aiming at the problem that sidelobe is easy to rise in the beam pattern of irregular array.

In this paper, a comprehensive optimized Taylor weighting algorithm and an overlapping array algorithm with reconfigurable subarrays are proposed to realize multipoint scanning and area coverage of cylindrical conformal array. The experimental results show that the sidelobe can be reduced from -11.27 dB to -18.66 dB when forming a single beam, from -3.3 dB to -15 dB when forming two beams with an interval of 30° and from -10.09 dB to -12.84 dB when forming two beams with an interval of 40°.

2. Cylindrical Conformal Array Model and Pattern Synthesis

The cylindrical conformal array antenna studied in this paper is divided into three layers with 144 array elements. Each layer including 48 uniformly distributed antenna elements with a height of 48 mm, and the radius of the cylinder is 280 mm as shown in Figure 1.

A sub-array in the cylindrical conformal array consists of 3 rows and 12 columns, and a total number of 36 elements are used for pattern synthesis as shown in Figure 2. Each TR module includes an IF input and three RF outputs as shown in Figure 3. The cylinder array patterns are synthesized and the simulation results are demonstrated in Figure 4.

Gain (G) is an index to measure the ability of the antenna to direct the power input to it in a specific direction, which is measured by the peak radiation intensity. Generally, the gain is related to the antenna pattern. The narrower the main lobe and the smaller the side lobe, the higher the gain. Assuming that the input power is P_0, the radiation power density of the omnidirectional antenna at the distance R is

$$S = \frac{P_0}{4\left(\pi R^2\right)}. \tag{1}$$

Since the omnidirectional antenna radiates uniformly in all directions, its radiation power density S is the radiation power divided by the sphere area, i.e., $4\pi R^2$. Assuming that the efficiency of the omnidirectional radiator is 100% and the electric field strength is E.

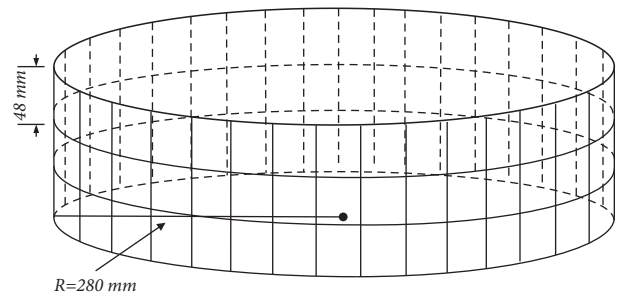

Figure 1: Cylindrical conformal array antenna consists of 3 layers, each layer containing 48 elements.

$$S = \frac{P_0 G}{4\pi R^2} = \frac{|E|^2}{\eta}. \tag{2}$$

Beamwidth is one of the parameters describing antenna performance, which refers to an antenna pattern or beam angle, in which the relative power is 50% or more of the highest power. Beamwidth refers to the angle at which the radiation power on both sides of the maximum radiation direction drops by 3 dB in the horizontal or vertical direction[21].

As shown in Figure 4, the three elements in the pitch direction form a wide beam with a sidelobe of -15.44 dB and a half-power beamwidth of 36°, which meets the pitch angle scanning requirement, and the sidelobe of the horizontal beam is -12.36 dB.

3. Sidelobe Optimization and Overlapping Array Division

The sidelobe level of the cylindrical conformal array is relatively high due to the influence of carrier curvature. In order to make the array antenna energy converge more in the main lobe pointing direction, the sidelobe suppression effect is optimized by amplitude "windowing." At the moment, the window functions mainly used are Chebyshev weighting and Taylor weighting [22]. Chebyshev weighting causes the excitation amplitude of the two end elements to jump when the number of array elements is large and the required sidelobe level is not very low. A minor error greatly affects the sidelobe level of the radiation pattern, which is not conducive to feeding. Taylor's weighted pattern shows that the sidelobe level in a certain area near the main lobe is nearly equal and monotonously decreases, which is beneficial to improve the antenna directivity coefficient. Meanwhile, the excitation amplitude distributions are monotonically decreasing from the array center to both ends with a proper design. There will be no jumping of excitation amplitude at both ends of the antenna, which is more suitable in the application scenario of multibeam forming. Therefore, Taylor optimization algorithm is used to suppress the sidelobe in this paper.

The traditional Taylor weighting technique is mainly suitable for uniform linear arrays and planar arrays with equally spaced array elements, while the existing nonuniform Taylor weighting algorithm only considers the nonuniform distribution in one-dimensional direction for sparse arrays based on linear arrays. The projection based on

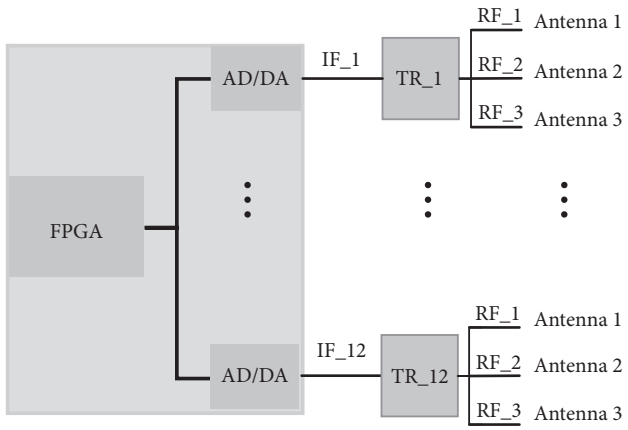

Figure 2: A sub-array of the cylindrical array.

conformal surface often ignores the influencing factors in nonhorizontal direction, which makes the sidelobe suppression effect nonoptimal. The Taylor function of discrete sampling continuous line source is used and projecteed in two-dimensional based on conformal array to normalize and weight the obtained two-dimensional optimization weights. Finally the comprehensive optimization weights matching the curvature of the conformal array are obtained, to further reduce the sidelobe of the cylindrical conformal array and raise the main lobe level.

A coordinate system is established based on a sub-array of a cylindrical array antenna, ignoring the pitching direction. Horizontal circular array with 48 elements evenly distributed, one sub-array contains 12 elements, and the two-dimensional projection is shown as Figure 5.

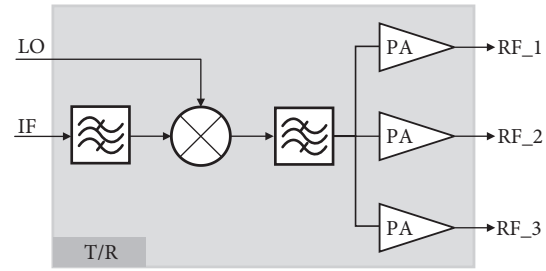

Figure 3: Each TR module has an IF input and three RF outputs, including filters, mixers and amplifiers.

In Figure 5, the projection of A_1 to A_{12}, i.e., 12 elements in a subarray, on the X axis is x_1 to x_{12}, while the projection of A_1 to A_6 on the Y axis is y_1 to y_6. The elements A_1 to A_6 with elements A_7 to A_{12} are symmetrically distributed around the Y axis.

The radius of the cylindrical array and the angle of the sector between A_1 and A_{12} are known to be r and θ_1, respectively. Then the chord length can be obtained through the formula $x_1x_{12} = 2r\sin(\theta_1/2)$. x_2x_{11} can be obtained through the formula $x_2x_{11} = 2r\sin(\theta_2/2)$ with the angle θ_2 correspondingly. The coordinates of 12 array elements projected on the X axis can be obtained. Note x_1x_{12} as d_1, x_2x_{11} as d_2, x_3x_{10} as d_3, x_4x_9 as d_4, x_5x_8 as d_5, and x_6x_7 as d_6. Therefore, it can be known that the projected nonuniform distribution coordinates on the X axis are $-d_1/2$, $-d_2/2$, $-d_3/2$, $-d_4/2$, $-d_5/2$, $-d_6/2$, $d_6/2$, $d_5/2$, $d_4/2$, $d_3/2$, $d_2/2$ and $d_1/2$, and the projection coordinates of the array elements on the Y axis can be obtained from the formula $r=(d^2+4h^2)/8h$.

The Taylor space factor is expressed as

$$\overline{S}(k) = \begin{cases} 1, k = 0 \\ \dfrac{[(\overline{n}-1)!]^2}{(\overline{n}+k-1)!\cdot(\overline{n}-k-1)!}\displaystyle\prod_{n=1}^{\overline{n}-1}\left\{1-\frac{k^2}{\sigma^2\left[A^2+(n-1/2)^2\right]}\right\}, & 1 \le k \le \overline{n}-1, \\ 0, k \ge \overline{n} \end{cases} \tag{3}$$

where R_0 means the ratio of the main lobe to side lobe level, $A = (\operatorname{arccosh} R_0)/\pi$ and $\sigma = \overline{n}/(\sqrt{A^2 + (\overline{n} - 1/2)^2})$. $\overline{n}$ means that the first $\overline{n}-1$ zeros of Taylor pattern are determined by the modified ideal space factor, so that the first $\overline{n}-1$ sidelobes are nearly equal. The general selection rule of $\overline{n}$ is $\overline{n} \ge 2A^2 + 1/2$, and here take $\overline{n} = 7$. Discretize the continuous Taylor space factor, as shown in Figure 6.

The current distribution on Taylor continuous line source antenna is as follows.

$$I(Z) = \frac{1}{L}\left[\overline{S}(0) + 2\sum_{k=1}^{\overline{n}-1}\overline{S}(k)\cos\left(\frac{2k\pi}{L}Z\right)\right]. \tag{4}$$

Ignoring the coefficient $1/L$ and make $\overline{S}(0) = 1$, the excitation amplitude of each unit of the discrete Taylor array is as follows.

$$I_n(Z_n) = 1 + 2\sum_{k=1}^{\overline{n}-1}\overline{S}(k)\cos(kp)], \tag{5}$$

where L is the total length of the linear array, here it is equal to d_1. It can be seen from Figure 5 that an equivalent transformation is required in the horizontal and vertical dimensions when the antenna elements of the conformal array are equivalent to linear arrays. In the horizontal direction, the coordinate matrix Z_n of the ordinary linear array with equal distance distribution is replaced by the nonuniform distribution coordinate Z_n' obtained by projection.

$$I_n(Z_n) = 1 + 2\sum_{k=1}^{\overline{n}-1}\overline{S}(k)\cos\left(k\frac{2\pi}{d_1}Z_n'\right). \tag{6}$$

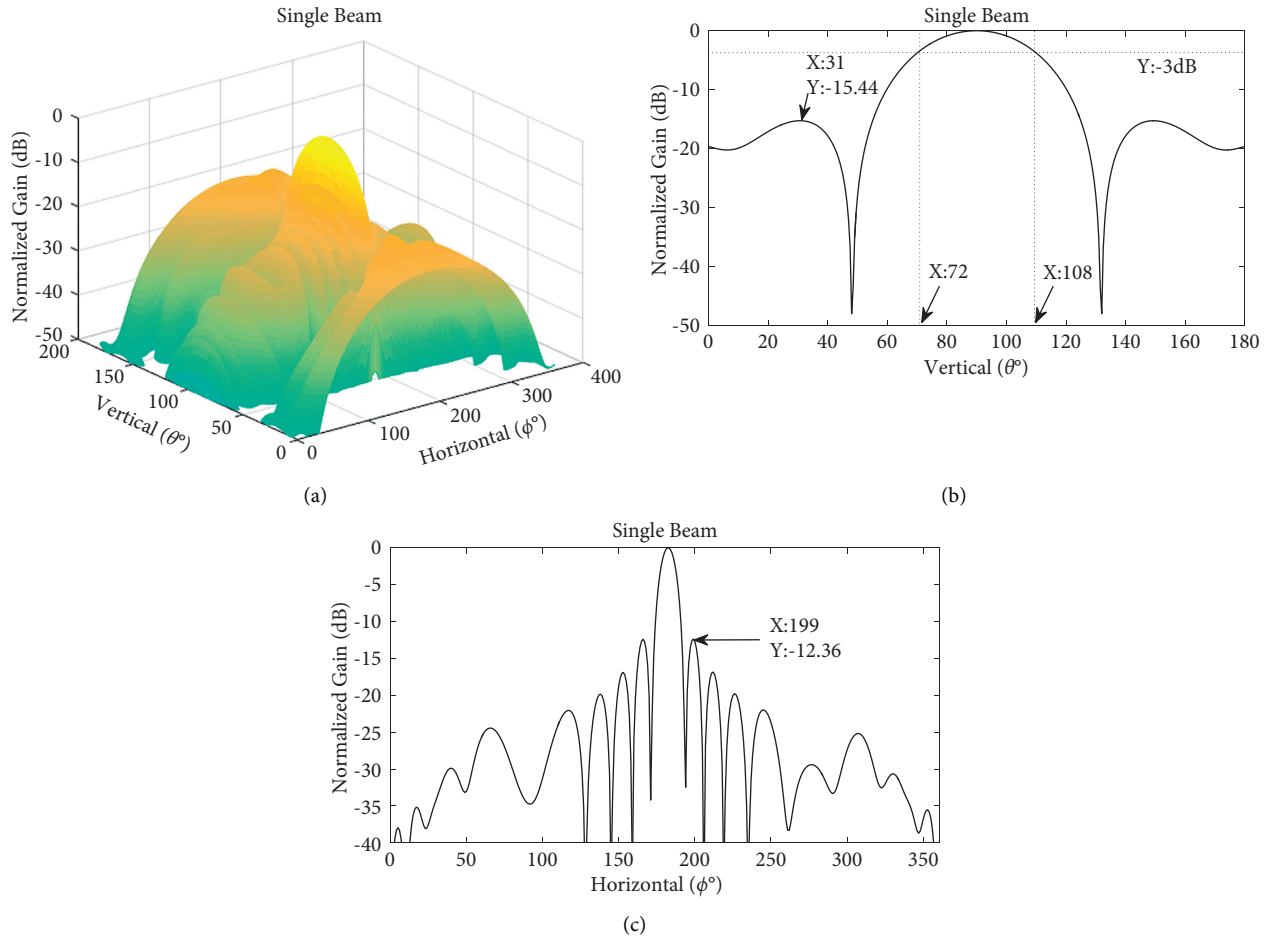

Figure 4: Pattern synthesis of cylindrical conformal array antenna: (a) 3D view, (b) elevation view, and (c) horizontal view.

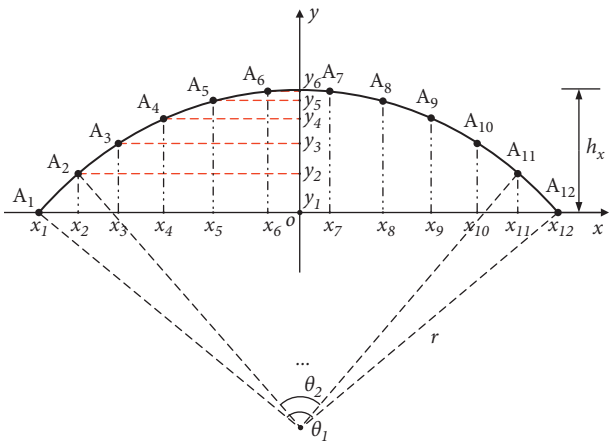

Figure 5: A sub-array of cylindrical conformal array in horizontal section, two-dimensional projection.

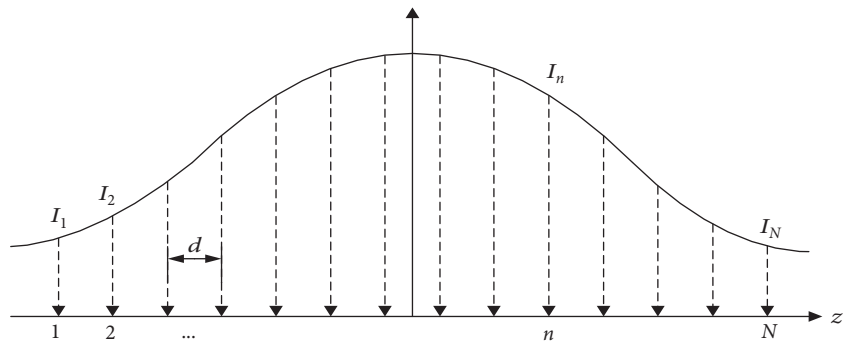

Figure 6: Discrete sampling of continuous Taylor function.

The current excitation amplitude $I_n(n = 1, 2, \ldots, 12)$ after horizontal nonuniform transformation is obtained from (4), while $I_6 = I_7, I_5 = I_8, I_4 = I_9, I_3 = I_{10}, I_2 = I_{11}$ and $I_1 = I_{12}$ according to the symmetry of conformal array. After normalizing the current excitation amplitude in the vertical direction according to different chord heights and integrating the influence factors of two dimensions, the Taylor current excitation amplitude after comprehensive optimization can be obtained as follows.

$$\begin{aligned}
I_{A6} &= I_{A7} = I_6,\\
I_{A5} &= I_{A8} = \frac{I_5 \cdot (R - y_6 y_5)}{R},\\
I_{A4} &= I_{A9} = \frac{I_4 \cdot (R - y_6 y_4)}{R},\\
I_{A3} &= I_{A10} = \frac{I_3 \cdot (R - y_6 y_3)}{R},\\
I_{A2} &= I_{A11} = \frac{I_2 \cdot (R - y_6 y_2)}{R},\\
I_{A1} &= I_{A12} = \frac{I_1 \cdot (R - y_6 y_1)}{R}.
\end{aligned} \tag{7}$$

Omni-directional multiangle multibeam forming in a cylindrical conformal array antenna needs to be done on the divided sub-array. Since the maximum gain of the subarray antenna unit cannot be completely obtained, the main lobe gain of the formed beam is low, the side lobe is high, and the beam pointing angle will be shifted to a certain extent, because the divided subarray sector is fixed and the main beam pointing is located in the sector edge. The main beam direction is random in actual beamforming due to the uncertainty of target signal orientation, which cannot guarantee the quality of the formed multibeam signal. To solve this problem, the divided subarray is set as Overlapping Subarray (OSA).

OSA can be divided into regular overlapping arrays and irregular overlapping arrays [23,24]. The division of overlapping arrays reduces the spacing between subarrays and increases the spacing of the grating lobes of subarrays. At the same time, OSA can reuse among array elements and can form sub-array patterns with "flat-top lobe" effect, thus effectively inhibiting the formation of grating lobes. On the basis of OSA, amplitude weighting is carried out. The diameter and the degree of freedom of the subarrays is increased without increasing the distance between the phase centers of the subarrays, making the calculation of beamforming more flexible [25]. Here, a multibeam forming method of OSA based on reconfigurable subarrays is proposed. On the basis of Taylor comprehensive optimization, it is different from the division method with a fixed number of OSA. The range of divided subarrays and the number of overlapping elements can be changed according to the main lobe direction, which can effectively narrow the main lobe, reduce the side lobe and suppress the grating lobe, and at the same time, form beams with high gain and accurate direction in different directions.

Multibeam forming based on reconfigurable subarrays is demonstrated in Figure 7.

Assume that the antenna element X is multiplexed n times in the overlapping array, its position in the first overlapping array is x_1, and its position in the n^{th} overlapping array is x_n. The Taylor comprehensive optimization weights of 12 elements are known as $[T_1, T_2, T_3, \ldots, T_{12}]$.

Then the weight of the antenna element X in the overlapping array N is shown as follows.

$$A_n = \frac{T_{x_n}}{T_{x_1} + T_{x_2} + T_{x_3} + \ldots + T_{x_n}}. \tag{8}$$

Equation (7) can be used to synthesize multibeam shaping for a cylindrical conformal array.

$$F(\varphi, \theta; \varphi_x, \theta_x) = \sum_{m=0}^{M-1} \sum_{n=0}^{N-1} f_{mn}(\varphi, \theta) A_{mn} \exp\{jkr_m [(sin\theta_m (sin\theta_x cos(\varphi_x - \varphi_{mn})) - sin\theta cos(\varphi - \varphi_{mn})) + cos\theta_m (cos\theta_x - cos\theta)]\}. \tag{9}$$

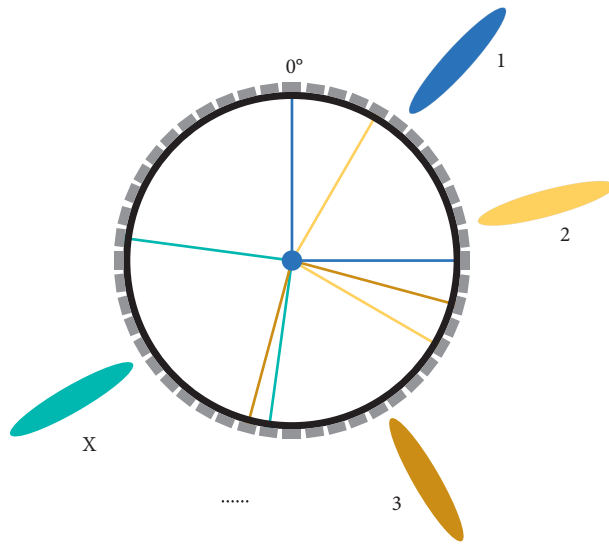

Figure 7: Multibeam forming of cylindrical array antenna based on overlapping array, and the subarray can be reconstructed.

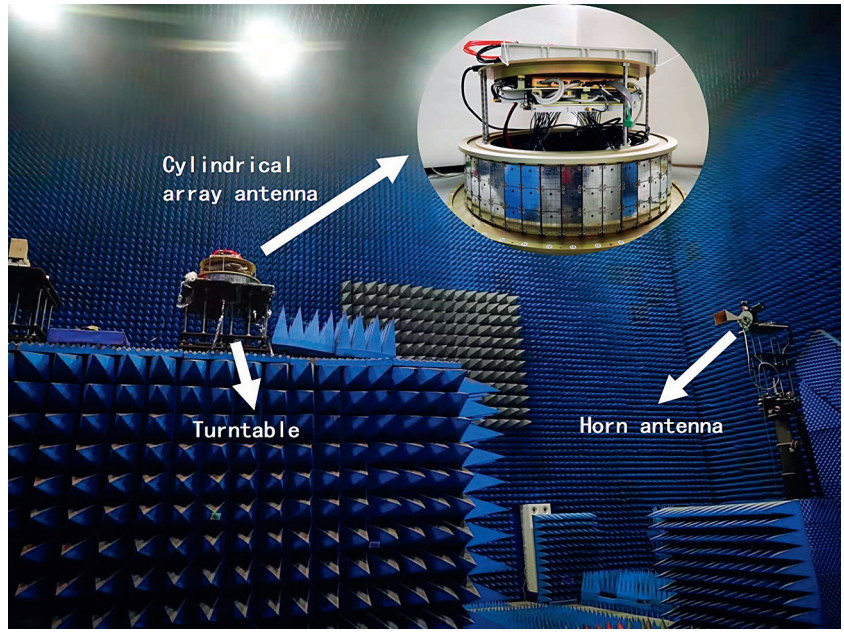

Figure 8: The pattern of cylindrical array antenna was tested in microwave anechoic chamber. There are 3×48 antenna units in the array and some hardware modules are exposed outside while in the preliminary debugging stage.

where $x = 0, 1, 2, \ldots X$, it means that X beams are formed. The directions of X beams are (φ_0, θ_0), (φ_1, θ_1), $(\varphi_2, \theta_2), \ldots, (\varphi_x, \theta_x)$ as shown in Figure 7. $f_{mn}(\varphi, \theta)$ represents the directed array element optimization function, where only horizontal scanning is considered. $f_n(\phi) = (1 + cos(\phi - \phi_n))/2$. As shown in Equation (9), A_{mn} represents the amplitude weighting coefficient after the simultaneous multibeam forming and Taylor optimization synthesis of the overlapping arrays.

$$A_n = \frac{1 + 2\sum_{k=1}^{\overline{n}-1} \overline{S}(k) cos\left(k2\pi/d_{x_n} Z'_{x_n}\right)}{\sum_{n=1}^{N}\left(1 + 2\sum_{k=1}^{\overline{n}-1} \overline{S}(k) cos\left(k2\pi/d_{x_n} Z'_{x_n}\right)\right)}. \quad (10)$$

4. Realization and Analysis of Multibeam Forming

The proposed beamforming algorithm is tested in a microwave anechoic chamber based on the designed cylindrical conformal array antenna prototype. The conformal antenna operates at 3.915 GHz and the test environment is shown in Figure 8.

Firstly, the pattern under the conditions of unoptimized traditional optimization and Taylor comprehensive optimization forming a single beam is tested. The measurement results are shown in Figure 9.

It can be seen from Figure 9 that the sidelobe of the single beam formed is -11.27 dB without optimization, the sidelobe

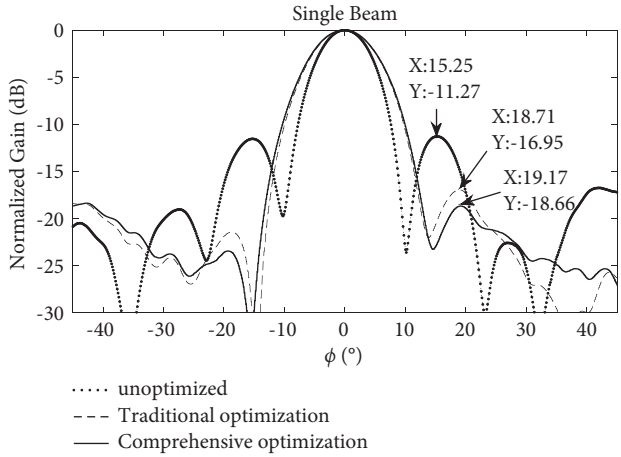

Figure 9: Single beam forming.

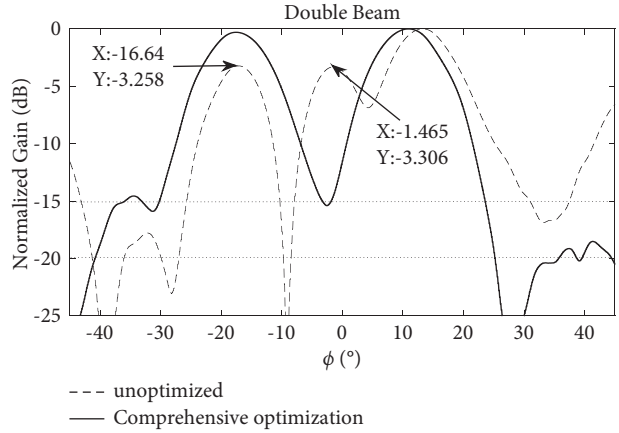

Figure 10: Two beams separated by 30°.

is -16.95 dB after optimization with traditional window function and the sidelobe is -18.66 dB after Taylor comprehensive optimization. It can be seen that the optimization algorithm will lead to a certain degree of broadening of the main lobe while reducing the side lobes, so it is necessary to set the optimization weight size according to the actual needs. The Taylor's comprehensive optimization can obtain lower sidelobes compared with traditional optimization from the figure, so Taylor's comprehensive optimization method is adopted to study the multibeam forming.

The experimental results before and after optimization are shown in Figure 10 when two beams separated by 30°. It can be seen that the main lobe of beam 1 is reduced by 3.258 dB by using the traditional structure to form two beams without optimizing by using the window function. The grating lobe appears between the two beams with a gain of -3.306 dB and the pointing direction of beam 2 is shifted. The two beams are separated by 30° with accurate pointing after optimization, while the left lobe is about -15 dB and the right lobe is about -20 dB.

The experimental results before and after optimization are as shown in Figure 11 when two beams separated by 40°. It can be seen that the left side lobe is -10.09 dB, the right side lobe is -16.6 dB, and the middle lobe of -13.65 dB with traditional structure to form two unoptimized beams. After

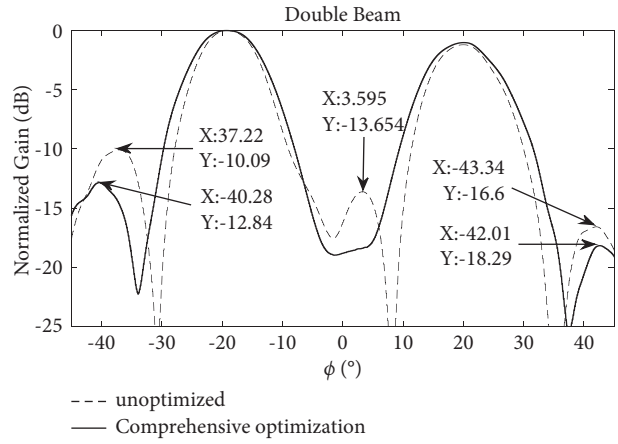

Figure 11: Two beams separated by 40°.

optimization, the left and right side lobes are reduced to -12.84 dB and -18.29 dB, respectively, and the middle grating lobe is eliminated.

At the end of this work, the peak sidelobe levels (PSLL) performance of several similar sidelobe optimization algorithms are compared, and the comparison results are shown in Table 1.

Table 1: Performance statistics of different algorithms in terms of PSLL.

Method	Lowest PSLL (dB)	Highest PSLL (dB)	Average PSLL (dB)
PSO in [18]	−10.06	−6.14	−7.68
NSFAII in [18]	−12.13	−9.04	−10.12
CO in [19]	−16.75	−12.995	−15.10
This work	−18.66	−23.5	−21.08

5. Conclusions

The multibeam forming algorithm of cylindrical conformal array antennas is studied in this paper. Based on Taylor's comprehensive optimization algorithm for sidelobe suppression, the overlapping array division method with reconfigurable subarrays is used to realize multibeam. Experimental results show that the algorithm can reduce the sidelobe by 7.39 dB in single beam forming scenario and accurately optimize the sidelobe level of each beam by 2–5 dB in multibeam forming, which proves that the algorithm can realize multibeam scanning of cylindrical conformal array.

Data Availability

The data used to support the findings of this study are available from the corresponding author upon request.

Conflicts of Interest

The authors declare that they have no conflicts of interest.

References

[1] T Zhou, J Huang, W Du, J Shen, and W Yuan, "2-D deconvolved conventional beamforming for a planar array," *Circuits, Systems, and Signal Processing*, vol. 8, no. 4, pp. 1–22, 2021.

[2] F. Sohrabi and W. Yu, "Hybrid digital and analog beamforming design for large-scale Antenna arrays," *IEEE Journal of Selected Topics in Signal Processing*, vol. 10, no. 3, pp. 501–513, 2016.

[3] X. F. Gao, P. Li, X. H. Hao, G. L. Li, and Z. J. Kong, "A novel DOA estimation algorithm using directional antennas in cylindrical conformal arrays," *Defence Technology*, vol. 17, no. 3, pp. 1042–1051, 2021.

[4] Y. Wang, J. Su, Z. Li, Q. Guo, and J. Song, "A prismatic conformal metasurface for radar cross-sectional reduction," *IEEE Antennas and Wireless Propagation Letters*, vol. 19, no. 4, pp. 631–635, 2020.

[5] S Guo, L. Zhang, Y. Wang, and C. Hu, "An accurate method for measuring airplane-borne conformal antenna's radar cross section," *Frequenz -Berlin-*, vol. 70, no. 9-10, pp. 397–401, 2016.

[6] B. Thors, L. Josefsson, and R. G. Rojas, "The RCS of a cylindrical array antenna coated with a dielectric layer," *IEEE Transactions on Antennas and Propagation*, vol. 52, no. 7, pp. 1851–1858, 2004.

[7] C. Fulton, J. L. Salazar, Y. Zhang et al., "Cylindrical polarimetric phased array radar: beamforming and calibration for weather applications," *IEEE Transactions on Geoscience and Remote Sensing*, vol. 55, no. 5, pp. 2827–2841, 2017.

[8] A Singh, S Vijay, and R. N Baral, "A review on development and analysis of conformal antennas for aircraft applications," *International Journal of Control Theory and Applications*, vol. 10, no. 9, pp. 1–10, 2017.

[9] L Wang, K Zhang, B Gao, M Wang, H Zheng, and E Li, "Conformal subgridding and application to one-eighth spherical shell dielectric resonator antenna array," *IEEE Transactions on Antennas and Propagation*, vol. 99, p. 1, 2020.

[10] C Bartram, R Henning, and D Primosch, "Demonstration of o-Ps detection with a cylindrical array of NaI detectors," *Nuclear Instruments and Methods in Physics Research Section A: Accelerators, Spectrometers, Detectors and Associated Equipment*, vol. 966, pp. 163856.1–163856.10, 2020.

[11] H Xu, J Cui, J Duan, B Zhang, and Y Tian, "Versatile Conical Conformal Array Antenna Based on Implementation of Independent and Endfire Radiation for UAV Applications," *IEEE Access*, vol. 7, pp. 31207–31217, 2019.

[12] O Elizarrarás, M. A Panduro, A Mendez, A Reyna, D. H Covarrubias, and L Garza, "Design of aperiodic spherical antenna arrays for wideband performance," *Annals Of Telecommunications - Annales Des Télécommunications*, vol. 12, no. 2, pp. 1–17, 2021.

[13] A. Durmus and R. Kurban, "Optimum design of linear and circular antenna arrays using equilibrium optimization algorithm," *International Journal of Microwave and Wireless Technologies*, vol. 13, no. 9, pp. 986–997, 2021.

[14] J.-W. Lian, Y.-L. Ban, H. Zhu, and Y. J. Guo, "Reduced-sidelobe multibeam array antenna based on SIW rotman lens," *IEEE Antennas and Wireless Propagation Letters*, vol. 19, no. 1, pp. 188–192, 2020.

[15] S Ma and X Mei, "Side-lobe constrained beamforming under virtual expansion of L-shaped array," *The Journal of China Universities of Posts and Telecommunications: English version*, vol. 28, no. 2, pp. 79–88, 2021.

[16] Y. Albagory, "Direction-independent and self-reconfigurable spherical-cap antenna array beamforming technique for massive 3D MIMO systems," *Wireless Networks*, vol. 26, no. 8, pp. 6111–6123, 2020.

[17] W. A Awan, A Zaidi, and M Hussain, "The Design of a Wideband Antenna with Notching Characteristics for Small Devices Using a Genetic Algorithm," *Mathematics*, vol. 9, p. 2113, 2021.

[18] H. Li, Y. Jiang, Y. Ding, J. Tan, and J. Zhou, "Low-sidelobe Pattern Synthesis for Sparse Conformal Arrays Based on PSO-SOCP Optimization," *IEEE Access*, vol. 6, pp. 77429–77439, 2018.

[19] F Yuan, B Yang, and Z. R Huang, "Joint optimization about pattern synthesis of circular arrays based on convex optimization and modified genetic algorithm," *Fire Control and Command Control*, vol. 40, no. 1, pp. 58–61, 2015.

[20] X. Ren, Y. Wang, and Qi Wang, "Beam optimization method based on radial basis function neural network," *Journal of Electronics and Information Technology*, vol. 43, no. 12, pp. 3695–3702, 2021.

[21] M. Mohammadi Shirkolaei, H. R. Dalili Oskouei, and M. Abbasi, "Design of 1∗4 microstrip antenna array on the

human thigh with gain enhancement," *IETE Journal of Research*, vol. 0, no. 0, pp. 1–7, 2021.

[22] G Guoqi Zeng, S Siyin Li, and Z Shanwei Lu, "Low side lobe pattern synthesis using projection method with genetic algorithm for truncated cone conformal phased arrays," *Journal of Systems Engineering and Electronics*, vol. 25, no. 4, pp. 554–559, 2014.

[23] Y. H Yu, Z. Y Zong, W Wu, Q Chen, and D. G Fang, "Dual-polarized linear array with overlapping handover of subarray to produce continuous beam scanning for transmitarray antenna," *IEEE Transactions on Antennas and Propagation*, vol. 69, pp. 859–868, 2020.

[24] T. Cheng, B. Wang, and L. Xia, "Inverse non-uniform overlapping subarray segmentation method of hybrid MIMO phased array radar," *Firepower and Command Control*, vol. 46, no. 1, pp. 25–31, 2021.

[25] X. Sheng, T. Liu, C. Yang, L. Guo, and M. Mu, "Joint DOA estimation method based on near-field nulling weight of subarray," *Journal of Electronics and Information Technology*, vol. 43, no. 3, pp. 727–734, 2021.